Excitons bound to neutral donors in InP

W. Rühle and W. Klingenstein
Physikalisches Institut—Teil 4—der Universität Stuttgart, Pfaffenwaldring 57, D-7000 Stuttgart 80—Federal Republic of Germany
(Received 9 May 1977)

Four sharp lines in very pure InP vapor-phase epitaxial layers are identified by absorption and luminescence experiments to be due to excitons bound to a shallow neutral donor in the $1S_{1/2}$ ground state. The symmetries of the three lower exciton states are determined by Zeeman spectroscopy to be Γ_8 (ground state), Γ_8, and Γ_7 (excited states). A simple model is proposed in which the excited states consist of a nonrigid rotation of light and heavy holes around the donor. In this model the energy spacings between excited and ground states are well understood.

I. INTRODUCTION

Hopfield[1] stated that neutral Coulomb-like impurities in semiconductors should always be able to bind excitons. While Hopfield gave only a qualitative dependence of the exciton localization energy on the ratio of the effective masses of electron and hole, several other authors[2-6] gave quantitative estimates of the localization energies as a function of the effective-mass ratio.

Experiments show, that in the case of direct-gap semiconductors with degenerate valence bands not just one, but several different lines are observed originating from the decay of excitons bound to shallow acceptors (A^0X) and donors (D^0X) even if only one specified impurity is present.[7-11] This splitting into different lines under zero-external-field conditions is well understood only in the case of the neutral acceptor complex.

It was explained, in particular through the work of White *et al.*,[11,12] by a j-j-coupling scheme for the three particles involved. The two holes couple together to a $J=0$ or $J=2$ Pauli-allowed state. When the electron is added, the $J=2$ state splits into a $J=\frac{3}{2}$ and a $J=\frac{5}{2}$ state, while the $J=0$ state leads to one $J=\frac{1}{2}$ state.[11-13]

Surprisingly, a splitting of the neutral-donor exciton states has been observed for several direct semiconductors, such as CdTe,[8] GaAs,[7] InP,[7,11] CdS,[9] and ZnSe.[10] This was not expected on the basis of the simple j-j-coupling model. Since the electron spins should be antiparallel, only one $J=\frac{3}{2}$ state due to the hole of the exciton is expected and therefore only one exciton line.[11]

It has been proposed that the electron-electron exchange in the D^0X state should be negligible in comparison to the electron-hole coupling.[14,15] One reason for this statement was the similar magnetic field splitting of two (D^0X) lines and the two free-exciton lines ($J=1$ and $J=2$) in CdTe.[14] However, the Zeeman splitting was measured without any polarization[14] and without quantitative evaluation, and similarities in the splitting pattern might be regarded as accidental. Indeed, Benoît à la Guillaume and Lavallard[16] drew attention to the fact that particularly the electron-electron exchange in Hopfields hydrogen-molecule picture produces the bound state, i.e., this exchange is not negligible at all. Therefore, they proposed a rigid-rotator model to explain the occurrence of these different D^0X lines at higher energies in CdTe.[16] In this model, the hole can be excited to a rotation around the fixed donor, i.e., a strong analogy to the rotation of diatomic molecules is assumed. However, this model, already proposed by Morgan,[17] does not explain the measured energetic distances between the different D^0X lines: In the case of InP and GaAs even no bound state is predicted for the $l=1$ rotational level of a rigid rotator, using the appropriate effective electron and hole masses and a reasonable distance[3] between the hole and the donor.

In general, Zeeman spectroscopy is a good means to elucidate the origin of lines, i.e., the symmetries of the initial and final states of the transitions. A Zeeman analysis has been performed in the case of the D^0X in CdTe,[8,14] InP,[11,18] and GaAs.[19] However, the interpretation of the data has not been conclusive. Until now neither the symmetries of all the D^0X states nor the transition schemes could be derived in an unambiguous manner.

In this paper we report for the first time a transition scheme for at least three of four observed D^0X lines in InP. This was possible after very carefully carrying out high-resolution Zeeman experiments in all possible polarizations (π, σ^+, σ^-; i.e., Voigt and Faraday configurations). InP is much more suitable for an experimental investigation of the D^0X lines than, e.g., GaAs, because a large zero-field splitting is observed. Extremely pure InP samples with different crystal orienta-

tions were used. It was necessary to perform emission as well as absorption measurements in order to overcome difficulties connected with thermalization of the initial states at the low temperatures used ($T < 2.1$ K). In order not to loose any of the magnetic-field-split components, the field had to be increased in very small steps of 0.2 T. Knowing the symmetries of the different D^0X states, the difficulties in former experimental works become understandable: As already indicated in Ref. 11, these D^0X states are extremely anisotropic, and the quadratic Zeeman effect plays an important role. The final state (in emission) is determined to be in every case the Γ_6 ($J=\frac{1}{2}$) level of a neutral donor with a g value of $g_e = 1.25$. Stress experiments confirm the symmetries determined by the Zeeman spectroscopy.

In knowledge of these symmetries we propose a simple modified rotational level scheme for the different D^0X states: Assuming a nonrigid rotator and taking into account the degeneracy of the valence band (heavy and light holes) the experimentally observed line distances and the appropriate degeneracy of the D^0X states can be well explained. The InP case should be taken as an ideal representative of the D^0X problem, the situation in CdTe, etc. should be similar.

II. EXPERIMENTAL

A. Samples

The best samples used were vapor-phase-epitaxial (VPE) layers grown on (100)-oriented substrates.[20] The carrier concentrations of the epitaxial layers were about 10^{13}–10^{14} cm^{-3}. Comparison of our VPE samples with high quality VPE samples grown at the Royal Signals and Radar Establishment (RSRE), St. Andrews Road, Great Malvern (doping level 1.6×10^{14} cm^{-3}, $\mu_{77\,K} = 101\,000$ V sec/cm^2), gave identical luminescence spectra. Different orientations[(110) and(111) surfaces] were also used for Zeeman spectroscopy, although these VPE layers were inferior in quality for these investigations.

For the absorption experiments, an optical window was etched into the sample by completely removing the substrate. A special etching method[21] was used to reduce the window thickness to about 10 μm. The use of thin samples was necessary, since absorption in the region of the D^0X complex in InP is very strong due to the beginning absorption of the free exciton.

B. Measurement techniques

1- and $\frac{3}{4}$-m grating spectrometers were used for the spectroscopic measurements. The samples were immersed in pumped liquid helium, also in the case of the temperature-dependent measurements. For the absorption measurements, a photomultiplier with S1 cathode (large dynamical range) was used. For the luminescence experiments a more sensitive GaAs cathode was taken. Normal lock-in technique was used for the amplification of the signals.

The magnetic field was produced by a split-coil superconducting magnet. Both Faraday and Voigt measurements were possible. The linear polarizers were HN7 Kodak polarization sheets. To distinguish right-circularly-polarized and left-circularly-polarized light in Faraday configuration a Fresnel rhomb in connection with a linear polarizer was used.

III. RESULTS AND DISCUSSION

A. Zero-field spectra

The lower part of Fig. 1 shows the low temperature (2 K) near the band-edge luminescence spectrum of one of the best InP samples at low excitation level (20 μW Ar$^+$ laser, focused to a spot of about 500 μm diam). Besides the free-exciton emission (FE) a series of four prominent sharp D^0X lines is observed. We label the lines 1–4 according to their energetic position, with line $(D^0X)_1$ lying at lowest energy. The energetic positions and their differences are compiled in Table I. The

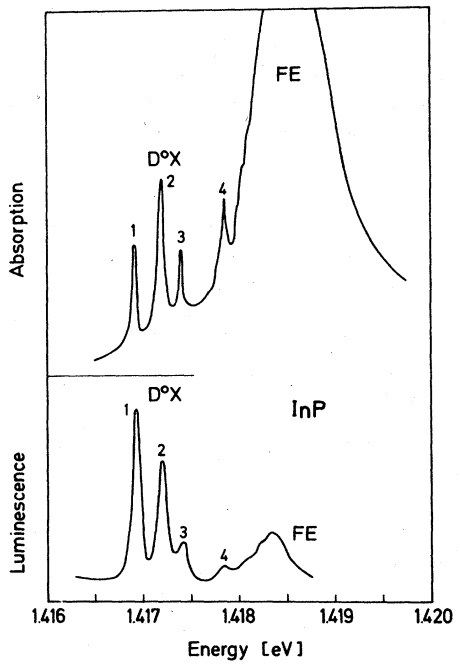

FIG. 1. Absorption (upper part) and luminescence spectra at the band edge of an InP epitaxial layer at low temperature ($T = 1.9$ K). The thickness of the absorption layer was about 10 μm.

TABLE I. In the first row the energetic positions of the four D^0X lines and the transverse free exciton energy (minimum of the free exciton reflection curve) are given. (1 eV = 1.239 513 3 × $10^4/\lambda$ Å). The second column compiles the energetical distances to line $(D^0X)_1$ and the third column gives the relative oscillator strengths as determined from the absorption spectra.

D^0X line	Energetic position (eV)	Energetic distance to $(D^0X)_1$ line (meV)	Oscillator strength ratio
1	1.416 92	···	1
2	1.417 19	0.273	2
3	1.417 40	0.483	0.77
4	1.417 84	0.925	0.96
FE	1.418 48	1.557	···

half-widths of the lines are extremely small (~0.04 meV).

The absorption of the same sample is shown in the upper part of Fig. 1. For different samples (n as well as p type) nearly the same intensity ratios (see Table I, last column) are observed for all four lines. This clearly demonstrates that they belong together and to only one species of binding center.

In emission, these intensity ratios are modified by thermalization effects: Figure 2(a) shows the intensity ratio of the four lines in emission plotted versus $1/T_{\text{bath}}$, where T_{bath} is the helium bath temperature. Although the lines show increasing thermalization effects in the sequence I_2–I_4, the activation energies obtained from this plot (ΔE_{21} = 0.15 meV, ΔE_{31} = 0.21 meV, ΔE_{41} = 0.28 meV) are too small and do not correspond to the optically determined line distances (compare Table I).

Especially, by extrapolating to $1/T \to 0$ we did not obtain the relative oscillator strength as determined by the absorption experiments. The situation becomes clearer if we plot the intensity ratio versus the reciprocal free-exciton temperature T_{FE} [Fig. 2(b)] instead of the reciprocal bath temperature. T_{FE} can be determined from the high-energy Boltzmann tail of the free-exciton emission (FE, Fig. 1). At a bath temperature of 1.96 K we obtain an exciton temperature of 3.14 K. In this "exciton temperature" scale the following activation energies are obtained:

$$\Delta E_{21} = 0.25 \text{ meV},$$

$$\Delta E_{31} = 0.43 \text{ meV},$$

$$\Delta E_{41} = 0.91 \text{ meV}.$$

These values are in reasonable agreement with the optically determined ones (compare Table I). We conclude that the bound excitons are at least partially in thermal equilibrium with the free exciton but not with the lattice which has the helium bath temperature at low excitation powers. This is not unreasonable since the lifetime of a D^0X state is extremely short (0.5 nsec).[22] Therefore, no complete exciton-lattice thermalization takes place before recombination.

All our results, especially the absorption experiments, demonstrate that the group of four D^0X lines belongs to one unique shallow donor-exciton complex with the binding donor being in the $1S_{1/2}$ ground state. No differences in the chemical

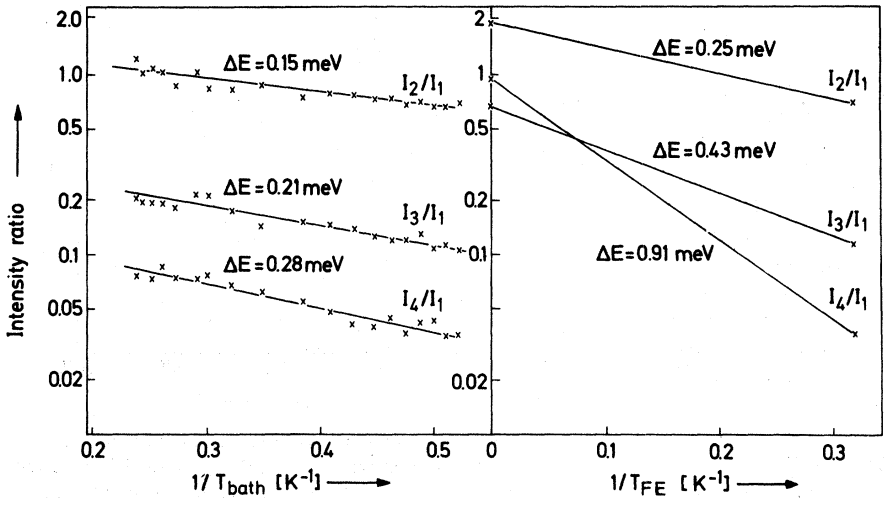

FIG. 2. Temperature dependence of the intensity ratios of the lines $(D^0X)_{2-4}$ with respect to line $(D^0X)_1$. On the left-hand side (a) these intensity ratios are plotted vs $1/T_{\text{bath}}$. We obtain the small activation energies given in the picture. On the right-hand side (b) the intensity ratios are given by taking the reciprocal free exciton temperature $1/T_{\text{FE}}$. These experimental points are connected with the intensity ratios for $1/T_{\text{FE}} \to 0$ as determined from the absorption experiments. The corresponding activation energies are given in the picture.

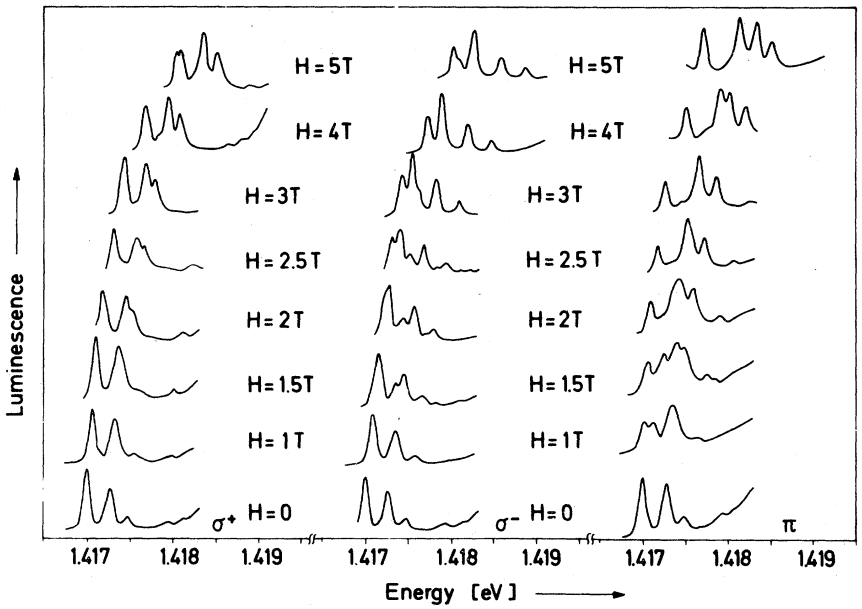

FIG. 3. Magnetoluminescence of the D^0X lines in InP with $H \| <100>$ in Voigt (π spectra) and Faraday (σ^+ and σ^- spectra) configuration. A splitting of the σ^+ and σ^- components of the lines $(D^0X)_1$ and $(D^0X)_2$ is observed at the following magnetic field strengths: $(D^0X)_1$: σ^+ ($\Delta m_j = -1$) at 5 T; σ^- ($\Delta m_j = +1$) at 2 T; $(D^0X)_2$: σ^+ at 2 T and σ^- at $H = 1.5$ T. The π components split already at 1 T, the upper component of line $(D^0X)_1$ crossing the lower component of line $(D^0X)_2$ between 2 and 3 T. The splitting of the lines $(D^0X)_{3,4}$ cannot be detected in luminescence.

nature of the donors cause the four different lines. This is in agreement with the earlier conclusions of White *et al.*[11] These authors already found that the three lower D^0X lines should belong to the same binding center.

B. Zeeman spectroscopy

Figure 3 shows the field-dependent D^0X luminescence for $H \| \langle 100 \rangle$ in π, σ^+, and σ^- polarization; Fig. 4, the corresponding spectra for absorption Figure 5 gives a fan chart as determined from both luminescence and absorption spectra in Figs. 3 and 4.

We observe that lines $(D^0X)_1$–$(D^0X)_3$ show a splitting into two π components (for line 3 see absorption spectra). Lines $(D^0X)_1$ and $(D^0X)_2$ split into two σ^+ and two σ^- components while line $(D^0X)_3$ shows only one σ^+ and one σ^- component. An earlier splitting pattern has been already given by White *et al.*[11] We obtain a complete polarization, which was not achieved under the experimental conditions of Ref. 11 if the sample is exactly oriented $H \| \langle 100 \rangle$. We suppose that stress effects in their experiments might have mixed polarizations. The final state in emission (initial state in absorption) is the twofold-degenerate Γ_6 ($J = \frac{1}{2}$) neutral-donor state. Therefore, one can conclude from the observed Zeeman splitting (four σ components) that the initial states $(D^0X)_{1,2}$ for lines 1 and 2 are fourfold-degenerate Γ_8 states ($J = \frac{3}{2}$) whereas for line 3 the initial state must be a twofold-degenerate Γ_7 state ($J = \frac{1}{2}$). The other possibility, that the $(D^0X)_3$ state has the twofold Γ_6 symmetry can be excluded since a Γ_6 to Γ_6 optical transition is forbidden for $H = 0$ and in magnetic fields only σ components should be observable for $H \| \langle 100 \rangle$.

We prove these assumptions by drawing transition schemes in Zeeman nomograms. This helpful means to elucidate the level scheme of transitions in Zeeman measurements was introduced by White *et al.*[23] Figure 6 gives an example at $H = 5$ T. The $(D^0X)_{1,2}$ and D^0 states are drawn on the

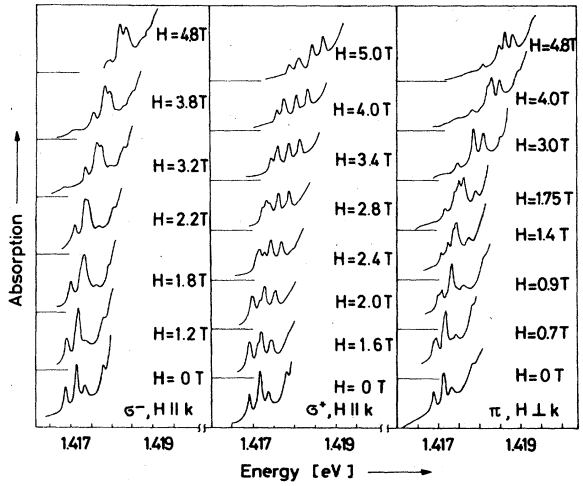

FIG. 4. Magnetoabsorption of the D^0X lines for Voigt and Faraday configuration. The splitting of the lines $(D^0X)_{1,2}$ corresponds to that one observed in emission spectra. No splitting of line $(D^0X)_3$ in σ^+ and σ^- polarization is observed (i.e., the $(D^0X)_3$ state must be a twofold degenerate Γ_7 state). The broadening of line 4 in the σ^+ and σ^- spectra might indicate a splitting, i.e., a higher degeneracy than a twofold one.

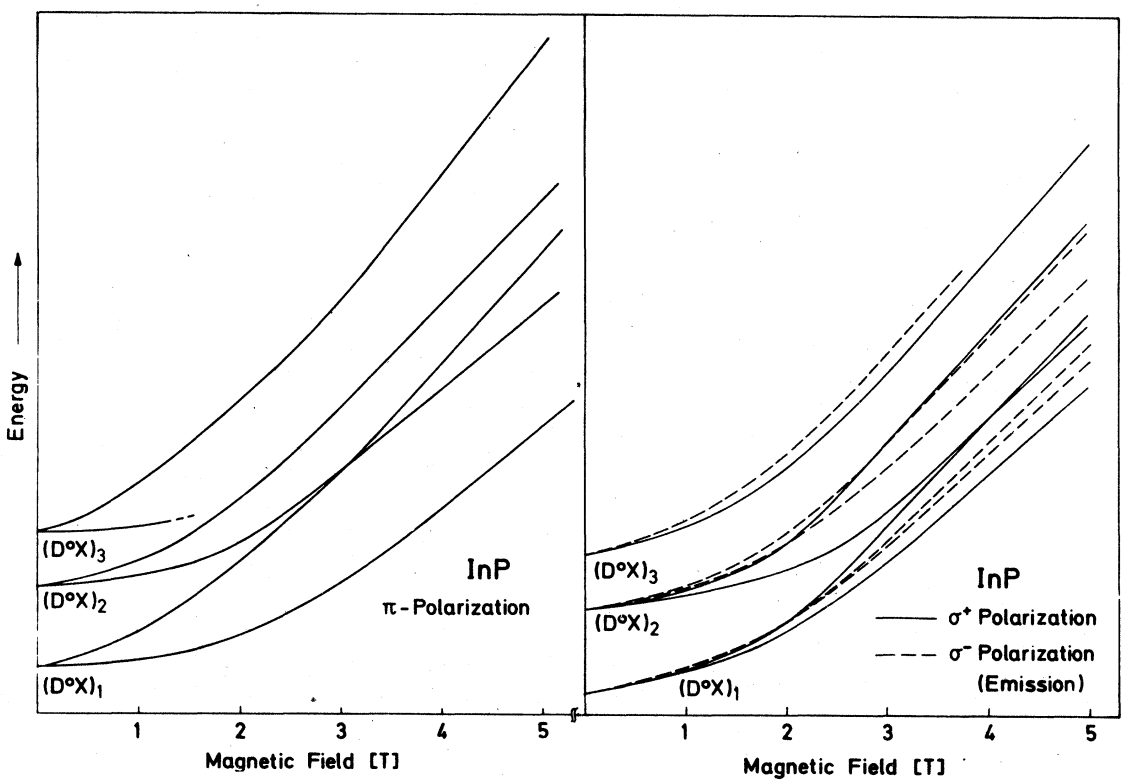

FIG. 5. Fan chart of the various Zeeman split components of the lower three $(D^0X)_{1-3}$ lines. For reasons of clearness the π spectra are drawn on the left-hand side, the σ spectra on the right-hand side. The change in m_j (in emission) is indicated at each line.

upper and lower lines with doubled energy scale in opposite directions. The position of the transition with the respective light polarization is marked on the middle line in a single energy scale. For characterizing the initial and final states we used the $|J, m_j\rangle$ labeling since for $H \| \langle 100 \rangle$ these are still good quantum numbers.[24] Transitions with $\Delta m_j = 0$ are π polarized, $\Delta m_j = \pm 1$ gives σ^- and σ^+ polarization. The following important results can be seen from this nomogram:

(i) Indeed we obtain for all lines the identical D^0 state with a g value of $g_e = 1.25 \pm 0.05$, which is in excellent agreement with other experiments.[25,26] (ii) The Γ_8 D^0X states must have large anisotropy: Please note that the $g_{1/2}$ and $g_{3/2}$ values for the $|m_j| = \frac{1}{2}$ and $|m_j| = \frac{3}{2}$ states are not only different $(\Delta E_{3/2} \neq 3\Delta E_{1/2})$ but have even opposite signs for both $(D^0X)_1$ and $(D^0X)_2$. (iii) Diamagnetic effects especially the so-called diamagnetic splitting play an extremely important role: The center of gravity of the $m_j = \pm\frac{1}{2}$ and $m_j = \pm\frac{3}{2}$ states is completely different: At $H = 5$ T (see Fig. 6) the latter lies 0.1 meV toward higher energies for both $(D^0X)_{1,2}$.

We were able to draw such nomograms for all magnetic fields measured, i.e., the identification of a line with the transition in the transition scheme is unambiguous. Furthermore, in σ polarization $(\Delta m_j = \pm 1)$ the intensity of a $m_j = \pm\frac{3}{2}$ to a $m_j = \pm\frac{1}{2}$ transition is 1.8 times more intense than the intensity of transitions from $m_j = \pm\frac{1}{2}$ to $m_j = \mp\frac{1}{2}$ states in both absorption and emission, after taking into account a proper thermalization. A theoretical ratio of 3:1 would be expected for these transitions.

From the observed linear Zeeman splittings, the isotropic $(\tilde{\kappa})$ and anisotropic $(\tilde{q})$ g values of the bound hole states can be determined. Using the formulas given in Ref. 24 we obtain for $H \| \langle 100 \rangle$

$$\tilde{\kappa} = \tfrac{1}{16}(-9g_{1/2} + g_{3/2}),$$
$$\tilde{q} = \tfrac{1}{4}(g_{1/2} - g_{3/2}).$$

The g values are compiled in Table II. Note the large anisotropy of the D^0X states: The anisotropic g value $\tilde{q}$ is nearly as large as the isotropic one $\tilde{\kappa}$. This was already observed by White *et al.*[11] We want to demonstrate this anisotropy even more directly by our experimental data:

In Fig. 7, Voigt spectra are shown with the $\vec{k}$ vector of light perpendicular to the (100) surface of the epitaxial layer. The sample is rotated in

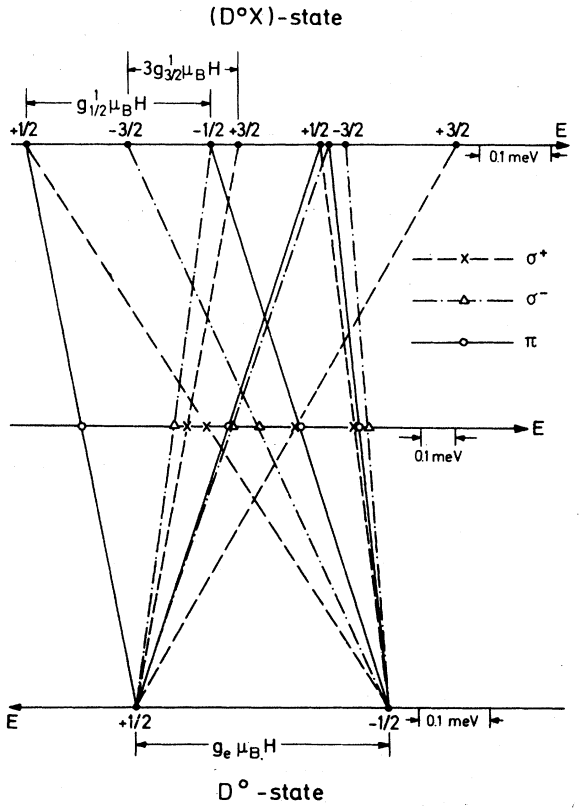

FIG. 6. Nomogram for the Zeeman splitting of the lines $(D^0X)_{1,2}$ at $H=5$ T with $H\|<100>$. The splitting of the $(D^0X)_{1,2}$ states are drawn in the upper horizontal line (doubled energy scale, increasing to the right), the splitting of the D^0 state is drawn in the lower line (doubled energy scale, increasing to the left side). On the middle line the experimentally observed lines with the respective polarization (for emission) are given (single energy scale, increasing to the right). The lines connecting the initial and final states intersect the middle line at the experimentally observed energetic positions. The excellent agreement between all the intersecting points and the experimental points for the case of the $m_j=\pm\frac{1}{2}$ states in π and σ polarization demonstrates that our transition scheme is correct.

TABLE II. g factors for the different D^0X states. The isotropic ($\tilde{\kappa}$) and anisotropic ($\tilde{q}$) g values are calculated from the observed splittings with $H\|\langle 100\rangle$; g^3 and $g^4_{1/2}$ are calculated from the splitting of the π-components of the $(D^0X)_{3,4}$ lines with $H\|\langle 100\rangle$, where g^3 is the g factor of the $\Gamma_7(D^0X)_3$ state and $g^4_{1/2}$ is the g factor of the $m_j=\frac{1}{2}$ states of line $(D^0X)_4$.

$\tilde{\kappa}_1$	0.508 ±0.03
$\tilde{q}_1$	0.280 ±0.03
$\tilde{\kappa}_2$	0.0466±0.03
$\tilde{q}_2$	−0.066 ±0.03
g^3	−1.3 ±0.15
$g^4_{1/2}$	−3.75 ±0.3

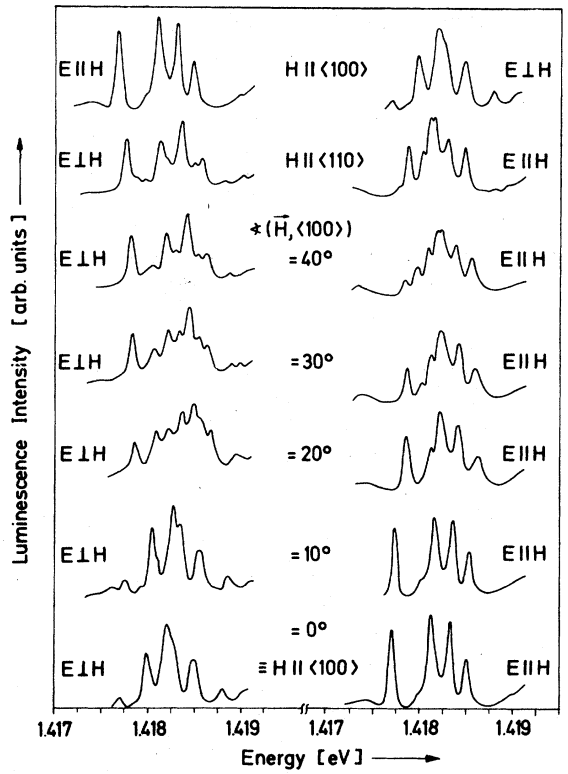

FIG. 7. Zeeman spectra at $H=5$ T in Voigt configuration with $\vec{k}_{light}\perp(100)_{sample}$. Going from the lowest to higher spectra the sample is rotated about the k vector. So the magnetic field orientation changes from $H\|<100>$ to $H\|<110>$ by a rotation of 45°. The uppermost spectra are once more with $H\|<100>$, but polarization between the left and right spectrums is interchanged.

this plane so that we change magnetic field orientation from $H\|\langle 100\rangle$ to $H\|\langle 110\rangle$ by a rotation with an angle of 45°. We observe a strong mixture of polarizations for intermediate positions. For $H\|\langle 110\rangle$ the σ spectrum is very similar to the π spectrum in the case of $H\|\langle 100\rangle$ as demonstrated by the two uppermost spectra. The reason is, that the $J=\frac{3}{2}$, $|m_j|=\frac{1}{2}$ state has changed the sign of the g value switching from $H\|\langle 100\rangle$ to $H\|\langle 110\rangle$.

The observed splitting with $H\|\langle 110\rangle$ and additionally with $H\|\langle 111\rangle$ offers a possibility to test whether the linear splitting of the $(D^0X)_{1,2}$ states is really that of a Γ_8 state: The group-theoretical treatment by Bhattacharjee and Rodriguez[27] connects the linear splitting of a Γ_8 state for magnetic fields parallel to the three different main crystal directions, $H\|\langle 100\rangle$, $H\|\langle 110\rangle$, and $H\|\langle 111\rangle$. Diagonalizing the matrices given for the linear Zeeman splitting with $H\|\langle 111\rangle$ and $H\|\langle 110\rangle$ in Ref. 27 we obtain the following numerical expressions for the g values:

$$H\parallel\langle 110\rangle \quad g_{1/2}=-2\tilde{\kappa}-5.388\tilde{q},$$
$$g_{3/2}=-2\tilde{\kappa}-4.129\tilde{q},$$
$$H\parallel\langle 111\rangle \quad g_{1/2}=-2\tilde{\kappa}-6.5\tilde{q},$$
$$g_{3/2}=-2\tilde{\kappa}-3.948\tilde{q},$$

where $g_{1/2}$ and $g_{3/2}$ are defined by $\Delta E_{1/2}=g_{1/2}\mu_B H$, the splitting of the $|m_j|=\frac{1}{2}$ levels, and $\Delta E_{3/2}=3g_{3/2}\mu_B H$, the splitting of the $|m_j|=\frac{3}{2}$ levels.

Please note that the m_j values are no longer good quantum numbers: The magnetic field mixes different m_j states for $H\parallel\langle 110\rangle$ and $H\parallel\langle 111\rangle$. Therefore, a mixing of polarization occurs and new transitions become allowed with increasing magnetic field.[24] (See, e.g., the π spectrum for $H\parallel\langle 110\rangle$ at $H=5$ T in Fig. 7: Six lines are observed instead of the four lines observed for $H\parallel\langle 100\rangle$.)

The g factors calculated with these formulas and with $\tilde{\kappa}$ and $\tilde{q}$ obtained from the splitting for $H\parallel\langle 100\rangle$ are shown in the first and third row of Table III. They must be compared with the experimentally determined values above them. The agreement is fairly good considering the large experimental uncertainty of the measured g-factors. This uncertainty is due to the following reasons: (i) Only samples with (100) surfaces show well-resolved spectra. (ii) Mixing of different m_j states with increasing magnetic fields produces more lines in the spectra and hence the identification of transitions is only possible at low magnetic fields and is not unambiguous.

The agreement in Table III confirms that the initial states of the lines $(D^0X)_1$ and $(D^0X)_2$ are really Γ_8 states. We note that on the other hand, this is the first experimental proof that the group-theoretical treatment of the linear splitting of Γ_8 states in magnetic fields by Bhattacharjee and Rodriguez[27] is still valid if these states are extremely anisotropic. The anisotropy, i.e., the large differences in the $g_{1/2}$ and $g_{3/2}$ factors might originate from the fact that the hole in the D^0X complex is bound very lightly, i.e., resembles a free hole. Calculating the valence-band Landau splitting with the newest valence-band parameters[26] it turns out, that the splitting ΔE of the lowest $m_j=\frac{1}{2}$ Landau states is comparable to that of the lowest $m_j=\frac{3}{2}$ states. Therefore, $g_{1/2}\neq g_{3/2}$ ($g_{1/2}\approx 3g_{3/2}$) for the lowest Landau levels. For $(D^0X)_1$, $g_{1/2}$ is approximately equal to three times $g_{3/2}$, i.e., the splitting of $(D^0X)_1$ states resembles that one of the lowest Landau levels. However, we still have no quantitative understanding of the large anisotropy of the D^0X states.

TABLE III. g factors for the $(D^0X)_{1,2}$ states for different magnetic field orientations. The calculated values for $H\parallel\langle 110\rangle$ and $H\parallel\langle 111\rangle$ are calculated from the observed splitting with $H\parallel\langle 100\rangle$. The experimental values for $H\parallel\langle 110\rangle$ and $H\parallel\langle 111\rangle$ are obtained from the π spectra at low magnetic fields.

		$H\parallel\langle 100\rangle$	$H\parallel\langle 110\rangle$	$H\parallel\langle 111\rangle$
$g^1_{1/2}$	expt	-0.876 ± 0.05	$+0.46\pm0.1$	$+0.65\pm0.1$
	calc		$+0.49$	$+0.80$
$g^1_{3/2}$	expt	$+0.245\pm0.05$		
$g^2_{1/2}$	expt	-0.06	$+0.24$	$+0.34$
	calc		$+0.26$	$+0.27$
$g^2_{3/2}$	expt	$+0.206$		

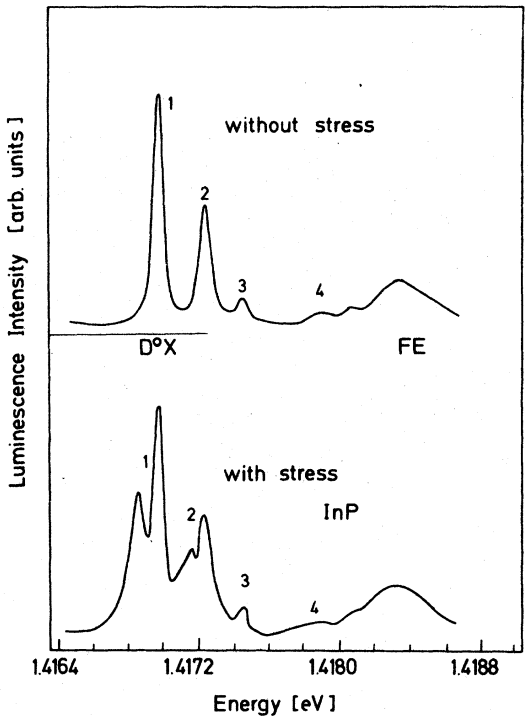

FIG. 8. Luminescence spectra with stress (lower) and without stress (upper). A clear stress splitting of the lines $(D^0X)_{1,2}$ is observed. Line $(D^0X)_3$ does not split; however, for line $(D^0X)_4$ a stress splitting is indicated.

We do not discuss the diamagnetic effects here, since we leave the low-field limit already at low magnetic fields. As well the diamagnetic shift as the diamagnetic splitting becomes nearly linear above 2.5 T. A phenomenological interpolation between the low- and high-field case—as proposed in Refs. 18 and 19—may be possible, but does not, however, provide new information.

Figure 8 demonstrates that the above assumed symmetries of the different D^0X states are supported by stress effects: Lines $(D^0X)_{1,2}$ clearly split into two components, i.e., the $(D^0X)_{1,2}$ states must be fourfold degenerate, whereas line $(D^0X)_3$ does not split, i.e., the $(D^0X)_3$ state is only two-

fold degenerate (Kramer's degeneracy). More carefully performed stress experiments[28] show identical results.

The splitting of line $(D^0X)_4$ cannot be resolved in all experiments (magnetic field and stress). However, in Fig. 8, the slight indication of a splitting (rather a broadening) of line $(D^0X)_4$ is observed which might demonstrate that the initial state of this transition should be at least fourfold degenerate. To summarize, the magnetic field dependence of the four D^0X lines demonstrates that—in emission—the *final* state is always a neutral donor. The *initial* $(D^0X)_{1,2}$ states are highly anisotropic, fourfold degenerate Γ_8 states whereas $(D^0X)_3$ is a twofold degenerate Γ_7 state. The stress splitting confirms these results and indicates that the initial state of line $(D^0X)_4$ is at least fourfold degenerate.

C. Ground and excited states of the D^0X complex

A basic and sophisticated quantum-theoretical treatment of the D^0X ground and excited states has been developed very recently by Herbert[6] but is so far unpublished. He performed variational calculations on the energetic positions of the D^0X complex with the hole in the $S_{3/2}$ ground state and in $P_{1/2}$, $P_{3/2}$, and $P_{5/2}$ excited states. For the case of GaAs it turned out that the $S_{3/2}$, $P_{3/2}$, and $P_{5/2}$ states should lie close together in energy, whereas the $P_{1/2}$ state of the hole should not be bound. Herbert's theoretical treatment should apply also to InP and yield basically similar results. Simultaneously, we have developed a more classical but very simple model in a Born-Oppenheimer approximation of an excitation of the hole into different, nonrigid-rotational states. A rigid-rotational model was originally proposed by Benoît à la Guillaume and Lavallard.[16] In principle, these rotational states ($\vec{l}=1$) correspond to the p-like distributions of the hole around the donor as proposed by Herbert.[6] After calculating the ground-state energy of the D^0X in the adiabatic approximation, as proposed by Sharma and Rodriguez[2] and Munchy,[3] we extend this approximation to the calculation of the first excited rotational level of the hole. In contrast to earlier estimates[16] we take into account the degeneracy of the valence band and that the hole rotation is nonrigid.

1. Calculation of the ground-state energy

Table IV gives a compilation of the valence-band effective masses of InP and GaAs. The table also contains the localization energies of the D^0X, determined after the theories of Munchy[3] (M) and Sharma and Rodriguez[2] (SR) using a mean hole mass as calculated from the effective-mass acceptor (EMA) (see Appendix). Finally, Table IV contains the experimentally determined localization energies: We took the energetical differences between the lowest D^0X line and the minimum of the reflection curve of the free-exciton polariton, which approximately corresponds to the transverse exciton energy.[29] The agreement between experimental and theoretical values is fairly good considering the uncertainty of the valence-band parameters and, last but not least, the approximations made in the theories (adiabatic approximation, no degeneracy of the holes).

The good agreement encourages us to assume that the adiabatic (Born-Oppenheimer) approximation, used in the calculations is not too bad, although the electron-to-hole mass ratios are not as small as one would require for such an approximation.

Before we discuss the rotational levels of the hole in this approximation, it should be mentioned

TABLE IV. Compilation of band parameters of InP and GaAs [m_e^* is the electron mass, m_{EMA}^* is the mean hole mass (see Appendix), m_{lh}^* is the light hole, m_{hh}^* is the heavy-hole effective masses]. The next columns give the localization energies determined experimentally and calculated after the theory of Munchy (M), or Sharma and Rodriguez (SR). The theoretical values for the rotational energy are the energy differences between the first excited ($I=1$) hole state calculated with heavy- and light-hole mass, respectively, and the $I=0$ hole ground state calculated with the mean hole mass m_{EMA}^*. The experimental values for the rotational energy are the energy difference between the center of gravity of the $(D^0X)_{3,4}$ lines and line 1 and the difference between the $(D^0X)_2$ line and the $(D^0X)_1$ line. ϵ_0 is the dielectric constant used in the calculations.

ϵ_0	InP 12.1 [a]	GaAs 12.5 [b]
m_{EMA}^*	0.495	0.299
m_{hh}^*	0.505 [c]	0.71 [c]
m_{lh}^*	0.126 [c]	0.081 [c]
E_{1ok}(M)[3] (meV)	1.51	1.39
E_{1ok}(SR)[2] (meV)	1.66	1.27
E_{1ok}(expt) (meV)	1.55	0.8
$l=1$ rotational energy, heavy hole		
theor	0.38	0.05
expt	0.28	0.06
$l=1$ rotational energy, light hole		
theor	1.00	0.77
expt	0.71	0.47

[a] P. J. Dean, A. M. White, E. W. Williams, and M. G. Astles, Solid State Commun. 9, 1555 (1971); note Ref. 11 therein.

[b] G. E. Stillman, C. M. Wolfe, and J. O. Dimmock, Solid State Commun. 7, 521 (1969).

[c] See Ref. 26.

that vibrational levels can be left out: For a H_2-like Morse-potential the first vibrational level already exceeds the localization energy, i.e., all vibrational levels are not bound.

2. *Calculation of the first nonrigid rotational level with $l = 1$*

Since the solution for rotational levels in case of a Morse potential is not easily calculated we use for this estimate another, more convenient form for an asymmetric attractive potential $V(r)$ as proposed by Kratzer[30]:

$$V(r) = -2D(a/r - a^2/2r^2) ,$$

where a is the distance hole-donor at the minimum potential energy D.

We are able to determine the quantities D and a for InP and GaAs from the calculations of Munchy.[3] No free parameter enters into the calculation. We obtain for the rotational levels E the following energies[31]:

$$E_l = \frac{-(2ma^2/\hbar^2)D^2}{\{0.5 + [(1+0.5)^2 + (2ma^2/\hbar^2)D]^{1/2}\}^2} ,$$

where l is the rotational quantum number and m the effective hole mass. This expression satisfactorily describes the situation for small quantum numbers l.

The idea is now, first to calculate the $l = 0$ rotational level with a mean effective hole mass (see Appendix). In the case of the $l = 1$ rotational level no mean but separately the light- or heavy-hole mass is used (and the corresponding values for the equilibrium distance a). The reason for this procedure is that for $l = 0$, (angular momentum $I = 0$) no direction of quantization is given, i.e., an isotropic mean-hole mass should be used. For $l = 1$ ($I = 1$), however, one has to distinguish between two cases: (i) The hole spin is oriented parallel or antiparallel to the quantizing axis of rotational angular momentum which means that the projection of the hole spin $\vec{j}$ on $\vec{I}$ is $m_j = \frac{3}{2}$ which is the m_j value for the light hole (perpendicular to $\vec{I}$). Therefore, the light-hole mass determines rotational energy. For these cases the total angular momentum is $J = \frac{1}{2}$ (antiparallel) or $J = \frac{5}{2}$ (parallel). (ii) The hole spin forms a certain angle to the $l = 1$ angular momentum which means that the projection of the hole spin $\vec{j}$ on $\vec{I}$ is $m_j = \frac{1}{2}$. In this case the heavy-hole mass determines rotational energy and the total angular momentum is $J = \frac{3}{2}$. This classification results in two rotational states: one with the heavy-hole mass at lower energies ($J = \frac{3}{2}$) and another one with the light-hole mass at higher energies ($J = \frac{1}{2}$ and $J = \frac{5}{2}$). The latter is split by a spin-orbit interaction into two levels with $J = \frac{1}{2}$ and $J = \frac{5}{2}$.

In terms of group theory for T_d symmetry, the coupling between a Γ_5 level ($\vec{I} = 1$) and the Γ_8 hole ($j = \frac{3}{2}$) results in one Γ_8 ($J = \frac{3}{2}$), one Γ_7 ($J = \frac{1}{2}$), and one $\Gamma_6 + \Gamma_8$ ($J = \frac{5}{2}$) state. To get a feeling whether these ideas go in the correct direction, we calculated the differences between the $l = 1$ rotational level and the $l = 0$ ground state as indicated above. For the two semiconductor materials InP and GaAs we obtained the values for the energy differences given in Table IV. These values must be compared with the experimentally measured differences between line $(D^0X)_2$ (Γ_8 state, heavy-hole mass) and line $(D^0X)_1$ and the difference between the center of gravity of lines $(D^0X)_3$ and $(D^0X)_4$ (Γ_7 and $\Gamma_6 + \Gamma_8$ states, light-hole mass) and the line $(D^0X)_1$. The agreement in both cases is nearly too good with respect to the simple models used.

We emphasize that the experimentally determined symmetry of $(D^0X)_2$, the lowest excited state, is indeed Γ_8, i.e. corresponds to a rotational level of the heavy hole. The sequence of the energy positions of the two predicted light hole levels with Γ_7 ($J = \frac{1}{2}$) or $\Gamma_6 + \Gamma_8$ ($J = \frac{5}{2}$) symmetry is not given by our simple model. Experimentally it turns out that the Γ_7 level lies at lower energy. In the more sophisticated theory of Herbert[6] the energetic sequence of the $P_{1/2}$ and $P_{5/2}$ levels does not agree with our experimental observation. This discrepancy is not understood at the moment.

Some comments should be made about some of the conclusions arising from this paper: (i) Rotational levels of the electron in case of the A^0X bound-exciton complex are difficult to observe for the following reasons: In this case the two heavier holes are localized at the acceptor and the light electron is bound by the Coulomb-potential of this A^+ state[4]: Rotation or better excitation into $2p$ states of the electron enlarges the electron wave function and hence reduces electron and hole overlap, i.e., the oscillator strength. (ii) The $l = 2$ rotational level of the D^0X is expected to appear only very weakly since the selection rules $\Delta l = \pm 1$ are still valid to a certain extent. Some of the weak lines observed at energies higher than that of line $(D^0X)_4$ might belong to such states.

IV. CONCLUSIONS

For the first time the symmetries of the ground $(D^0X)_1$ state and two excited $(D^0X)_{2,3}$ states for a direct-gap III-V compound with degenerate valence band could be determined. We developed a simple but very clearly understandable model for the excited states of the hole in a D^0X complex:

A nonrigid rotation of the hole around the donor is calculated within an adiabatic approximation. If the degeneracy of light and heavy holes is as-

sumed to be lifted in the first excited p-like state, we get a good agreement between the experimentally observed and theoretically calculated energy spacings between the ground and the excited states. A more general theoretical treatment of the problem will be published by Herbert.[6]

ACKNOWLEDGEMENTS

The financial support of the Deutsche Forschungsgemeinschaft in the framework of the SFB 67 is gratefully acknowledged. We are grateful to M. Pilkuhn, J. U. Fischbach, D. Bimberg, K. Hess, and J. Weber for their contributions to this paper, particularly for stimulating discussions. Many thanks are due to P. Rossetto and the other co-workers of the Stuttgart crystal laboratory, who grew the very pure InP samples used for the experiments reported here.

We thank D. C. Herbert (RSRE, Malvern) for giving us a preliminary unpublished version of his theoretical treatment of the bound exciton problem prior to publication. We finally thank our colleagues at the RSRE, Malvern, for the InP reference samples.

APPENDIX:

"Mean" hole mass in the (D^0X) ground state Baldereschi and Lipari[32] developed a spherical model of the acceptor state in cubic semiconductors with degenerate valence band. It turned out that not only the isotropic valence band mass ($m = 1/\gamma_1$, where γ_1 is the Luttinger parameter) determines the hole binding energy but also the separation into light- and heavy-hole masses (Luttinger parameter γ_2). With increasing differences in light- and heavy-hole masses the ionization energy increases strongly. The heavier hole has more influence on the binding energy than the light hole. We assume in this paper, that in the case of the D^0X ground state the "mean" effective-hole mass which determines the localization energy should correspond to the mean hole mass which determines the hole binding energy in the case of an effective-mass acceptor (EMA). This mass m^*_{EMA} is calculated from the acceptor ionization energy E_{EMA}, assuming a hydrogenlike formula,

$$m^*_{\mathrm{EMA}} = \frac{E_{\mathrm{EMA}}}{13.6\epsilon^2 \times 10^3 \text{ meV}} ,$$

where ϵ is the static dielectric constant.

With the newest valence-band parameters for GaAs and InP,[26,28] and the theory of Baldereschi and Lipari,[32] we obtain the following ionization energies of the EMA:

for InP: $E_{\mathrm{EMA}} = 46$ meV,

for GaAs: $E_{\mathrm{EMA}} = 26$ meV.

With these values and the formula above we obtain the mean effective-hole masses given in Table IV.

[1] J.J.Hopfield, in *Proceedings of the International Conference on the Physics of Semiconductors, Paris, 1964,* edited by M. Hulin (Dunod, Paris, 1965), p. 725.
[2] R. R. Sharma and S. Rodriguez, Phys. Rev. 159, 649 (1967).
[3] G. Munchy, J. Phys. (Paris) 28, 307 (1967).
[4] D. S. Pan, D. L. Smith, and T. C. McGill, Solid State Commun. 18, 1557 (1976).
[5] G. Munchy and C. Carabatos, Phys. Status Solidi B 57, 523 (1973).
[6] D. C. Herbert (unpublished).
[7] A. M. White, P. J. Dean, L. L. Taylor, R. C. Clarke, P. J. Ashen, and J. B. Mullin, J. Phys. C 5, 1727 (1972).
[8] P. Hiesinger, S. Suga, F. Willmann, and W. Dreybrodt, Phys. Status Solidi B 67, 641 (1975).
[9] C. H. Henry and K. Nassau, Phys. Rev. B 2, 997 (1970).
[10] J. L. Merz, H. Kukimoto, K. Nassau, and J. W. Shiever, Phys. Rev. B 6, 545 (1972).
[11] A. M. White, P. J. Dean, and B. Day, J. Phys. C 7, 1400 (1974).
[12] A. M. White, J. Phys. C 6, 1971 (1973).
[13] Martin Schmidt, T. N. Morgan, and W. Schairer, Phys. Rev. B 11, 5002 (1975).
[14] K. Cho, W. Dreybrodt, P. Hiesinger, S. Suga, and F. Willmann, in *Proceedings of the Twelfth International Conference on the Physics of Semiconductors, Stuttgart, 1974,* edited by M. H. Pilkuhn (Teubner, Leipzig, 1976), p. 945.
[15] N. Stath, thesis (University of Stuttgart, 1974) (unpublished).
[16] C. Benoît à la Guillaume and P. Lavallard, Phys. Status Solidi B 70, K143 (1975).
[17] T. N. Morgan (private communication).
[18] D. C. Reynolds, C. W. Litton, R. J. Almassy, S. B. Nam, P. J. Dean, and R. C. Clarke, Phys. Rev. B 13, 2507 (1976).
[19] D. C. Reynolds, C. W. Litton, T. C. Collins, S. B. Nam, and C. M. Wolfe, Phys. Rev. B 12, 5723 (1975).
[20] P. Rossetto *et al.* (unpublished).
[21] W. Klingenstein (unpublished).
[22] U. Heim, Phys. Status Solidi B 48, 629 (1971).
[23] A. M. White, P. J. Dean, D. J. Ashen, J. B. Mullin, and B. Day, in Ref. 14, p. 381; R. A. Fischer and S. Goudsmit, Phys. Rev. 37, 1057 (1934).
[24] W. Schairer, D. Bimberg, W. Kottler, K. Cho, and Martin Schmidt, Phys. Rev. B 13, 3452 (1976).
[25] C. Weisbuch, C. Hermann, and G. Fishman, in Ref. 14, p. 761.
[26] D. Bimberg, K. Hess, N. O. Lipari, J. U. Fischbach, and M. Altarelli, in *Proceedings of the International Conference on Magneto-Optics, Zurich, 1976,* edited

by P. Wachter (North-Holland, Amsterdam, 1977), p. 139.
[27]A. K. Bhattacharjee and S. Rodriguez, Phys. Rev. B 6, 3836 (1972).
[28]K. Hess, thesis (University of Stuttgart, 1976) (unpublished).
[29]F. Evangelisti, J. U. Fischbach, and A. Frova, Phys. Rev. B 9, 1516 (1974).
[30]A. Kratzer, Z. Phys. 3, 289 (1920).
[31]S. Flügge, *Rechenmethoden der Quantentheorie* (Springer-Verlag, Berlin, 1965).
[32]A. Baldereschi and Nunzio O. Lipari, Phys. Rev. B 8, 2697 (1973).